CREEP BEHAVIOR OF A DIRECTIONALLY SOLIDIFIED NICKEL BASED SUPERALLOY

Alejandro R. Ibañez[1] Ashok Saxena[2] and JiDong Kang[3]
[1] INVAP SE, Moreno 1089, S.C. de Bariloche, 8400, Argentina
[2] College of Engineering, University of Arkansas, Fayetteville, AR, USA
[3] Department of Materials Science and Engineering, McMaster University, Hamilton, Canada

ABSTRACT

Directionally solidified nickel-base superalloys provide significant improvements relative to the limitations inherent to equiaxed materials in the areas of creep resistance, oxidation, and low and high cycle fatigue resistance. The objectives of this study are to perform critical experiments and investigate the high temperature creep deformation, creep rupture and creep crack growth behavior of DS GTD111. The specimens in the longitudinal direction showed higher creep ductility, lower minimum strain rates and longer creep rupture times than the specimens in the transverse direction. The results in the transverse direction were similar to the ones for the equiaxed version of this superalloy A power-law model and the theta-projection model is evaluated for representing the material behavior and both appear to provide accurate representations of creep deformation over a wide range of stress, time and temperature conditions. The Monkman-Grant relationship, the Larson-Miller parameter and the theta projection model have been successfully used to predict the time to rupture for different orientation-temperature-stress conditions. The time dependent fracture mechanics approach is used to model creep crack growth behavior.

1 INTRODUCTION

The energy conversion efficiencies of natural gas-fired turbines has steadily improved with developments in the temperature capability of advanced materials for hot gas path components. The use of directionally solidified (DS) superalloy with adequate coatings has significantly improved the limitations inherent to equiaxed materials in the areas of oxidation and corrosion resistance, thermal and low cycle fatigue resistance, creep resistance and high cycle fatigue resistance, Woodford & Stiles [1]. Accurate mathematical models are needed to predict the service lives of hot-section components to prevent unscheduled outages due to sudden failures. The goals of this research are (a) to perform critical experiments and investigate the high temperature, creep deformation, creep rupture and creep crack growth behavior of DS GTD111 and b) to develop mathematical models for representing the above behavior.

2 EXPERIMENTAL PROCEDURE

To meet the objectives of this study, creep deformation and rupture tests and creep crack growth tests were conducted.

The material to be analyzed is a DS nickel based superalloy with a nominal chemical composition shown in Table 1. Rectangular test blocks of constant thickness from DS GTD111 were specially cast because they are most suitable in size and shape for machining large number of specimens. The grains were oriented along the length of the test blocks. The material was received in two batches. Although the heat treatments were nominally the same, the potential exists for variability in the microstructure. The Rockwell C hardness values of the material from the two batches was quite similar. For Batch 1, the average hardness measured was 39.6 with a deviation of ± 1.5. For Batch 2, the average was 40.0 and the deviation was ± 1.2.

The microstructure of DS GTD111 was reported to be similar in terms of grain size, γ' particle size and secondary dendrite arm spacing (SDAS) for material from both batches. The typical

grain width has been reported by Trexler & Sanders [2] to be 5.1 mm and the grain length 140 mm. The coarse γ' precipitates have been reported to be cubes of about 1 μm side while the fine γ' precipitates spheres with diameters between 0.14 and 0.24 μm. The γ' particles located within a dendrite are smaller in size than the particles located in the interdendritic region.

Table 1: Nominal chemical composition of the superalloy used in the study

	Cr	Co	Al	Ti	W	Mo	Ta	C	Zr	B	Fe	Si	Mn	Cu	P	S	Ni
Min	13.7	9.0	2.8	4.7	3.5	1.4	2.5	.08	.005	-	-	-	-	-	-	-	Bal
Max	14.3	10.0	3.2	5.1	4.1	1.7	3.1	.12	.040	.02	.35	.30	.10	.10	.015	.005	Bal

The specimens utilized for the creep deformation and rupture tests were 25.4 mm long and 4.064 mm in diameter. A lever-type, dead-weight creep machine was used to apply the load to the specimens. The ratio of the lever arms was 20:1. A three zone, electric resistance furnace was used to heat the specimens to their test temperature and maintain it within ± 1°C of the desired value. The displacement was measured continually using a high temperature extensometer securely mounted on the specimens with the aid of screws inserted in the small holes machined in the specimens. The displacement in the extensometer was measured outside the furnace with a high precision capacitance gage. The displacement and temperature were logged continually with a digital recorder until the specimen under test fails. The temperature was measured with two K-type thermocouple directly attached to the specimen in different parts of the gage area.

The creep crack growth tests were conducted using the compact type C(T) specimens with width of 50.8 mm and thickness of 12.7 mm. The specimens were side-grooved with depths of 10% of the thickness on each face of the specimen to prevent out of plane crack growth during the test. The initial crack size to width ratio (a/W) was about 0.50. A lever-type, dead-weight creep machine was used to apply the load to the specimens. A three zone, electric resistance furnace was used to heat the specimens to their test temperature and the temperature was maintained to within ± 1ºC. Temperature was measured with two K-type thermocouples welded to each C(T) specimen. For tests at 761°C or below the load-line displacement at any instant was measured with a high temperature extensometer attached to the knife edges machined onto the C(T) specimen. The displacement in the extensometer was measured outside the furnace with a high precision capacitance gage. For tests above 761°C, the load line displacement was continuously measured at the lever arm with a high precision capacitance gage. The crack length was measured at all times during the tests using the direct potential drop technique. Most of the tests were terminated before final fracture. The tested specimens were cracked open at room temperature by applying fatigue loads to extend the crack until failure. The final crack length and the precrack lengths were measured at nine points evenly spaced in the thickness direction. In case the measured final crack length was different from that predicted by the DC potential method, the predicted crack length was corrected using a linear distribution of error. The displacement, output voltage and temperature were logged continually in a digital recorder until the test is stopped.

3 RESULTS & DISCUSSION

3.1 Creep Deformation and Rupture

The creep deformation behavior consistently shows a very short primary creep regime, followed

by a substantial steady-state region that accounts for more than half of the creep life but only between 20% and 33% of the creep strain (see Figure 1). The last portion of the creep curve is characterized by tertiary creep, which is responsible for less than half of the creep life but for the majority of the accumulated creep strain. As can be seen in Figure 1, specimens from Batch 1 have shorter creep lives at the same stress level in comparison to ones from Batch 2. They also have lower ductility and higher minimum strain rate. The difference in creep deformation behavior between the longitudinal and transverse orientations decreases with increasing temperature. Comparing results from tests performed at the same temperature and stress but different orientations it is noticed that at a certain stress at 871°C the time to rupture in the longitudinal direction is 1.38 times longer than in the transverse direction. This factor increases to 2.5 for 815°C, 5.7 for 760°C and over 400 for 649°C. The trend suggests that at temperatures above 871°C, the difference could become even smaller. The final creep elongation for each specimen was measured with a traveling microscope by joining two halves of the fractured specimen after it was removed from the load frame. In general, the tests in longitudinal direction exhibit higher elongations compared to the ones in the transverse direction and the elongation appears to increase with temperature and with stress. However, there are some exceptions to this behavior. The elongations ranged from a low of approximately 2% to a high of almost 25%.

The power law creep model describes the creep behavior of a material utilizing eqn. (1), [3][4]

$$\dot{e} = As^{n} + A_3 s^{n_3} e_{TC}^{\,p_3} \tag{1}$$

where, $\dot{e}$ = strain rate, s=applied stress and A, A_3, n, n_3 and p_3 are regression constants and ε_{TC} is the instantaneous tertiary creep strain. The values of A and n obtained from regression are provided in Figure 3. According to the model n is considered to be independent of temperature, and A is assumed to have an Arrenhius type relationship with temperature. The value of A is plotted versus *1/T* on a semi-log scale in Figure 3. It can be seen that the straight lines for both orientations are parallel between 760°C and 871°C. For the longitudinal orientation, the linear trend continues to 982°C. The activation energy for the process, Q, above 760°C was calculated to be 3773 *KJ/mol* in the longitudinal case and 3636 *KJ/mol* for the transverse. The values of n for different temperatures are also plotted in Figure 3. It can be seen that n varies with temperature in a manner similar to A. Therefore we can model this behavior as linear and predict the minimum strain rate for any temperature-stress combination. Once this minimum strain rate is obtained, the Monkman-Grant [5] criterion, $\log t_R + m \log \dot{e}_{ss} = constant$, could be coupled with it to predict the rupture behavior of this alloy. This result can be seen in Figure 2.

The q-projection method was introduced by Evans & Wilshire [6], which fully describes the creep strain *vs*. time behavior by means of the following equation

$$e = q_1(1 - e^{-q_2 t}) + q_3(e^{+q_4 t} - 1) \tag{3}$$

where q_I are fitting constants and their natural logarithm has a linear behavior with temperature and applied stress. This model was used to predict the creep strain as a function of time for any combination of temperature and applied stress with accuracy. Furthermore, by taking the derivative of eqn. (3) we obtain the strain rates. Using the rupture criterion that the specimen fails when the strain rate is larger than a critical strain rate we can predict the creep life of the specimen. Those results can be seen in Figure 2.

The Larson-Miller parameter (LMP) (Larson & MIller [7]) is calculated by: $LMP = T(Log\ t_R + 20)$, where T is temperature and t_R the time to rupture. For a given material, a plot of stress versus *LMP* results in a single plot regardless of the time-temperature combination employed to derive the parameter. The LMP for equiaxed GTD111 reported by Viswanathan[8] is comparable to the rupture lives in the transverse direction. In Figure 2 the stress *vs.* time to rupture at different

temperatures obtained from the *LMP* is plotted for the longitudinal and transverse orientation. To generate the curves a cubic polynomial was used to fit the stress vs. *LMP* behavior. It can be seen that the predicted times to rupture by this model are in good agreement with the experimental data in the investigated range of temperatures and stresses.

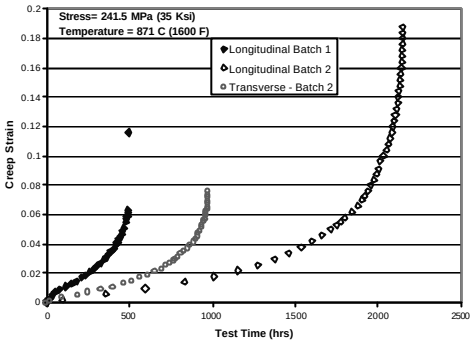

Figure 1: Direct comparison of creep deformation and rupture behavior of DS GTD111 in the longitudinal and transverse direction and between specimens from Batch 1 and Batch 2 materials at a stress level of 241.5 MPa (35 Ksi).

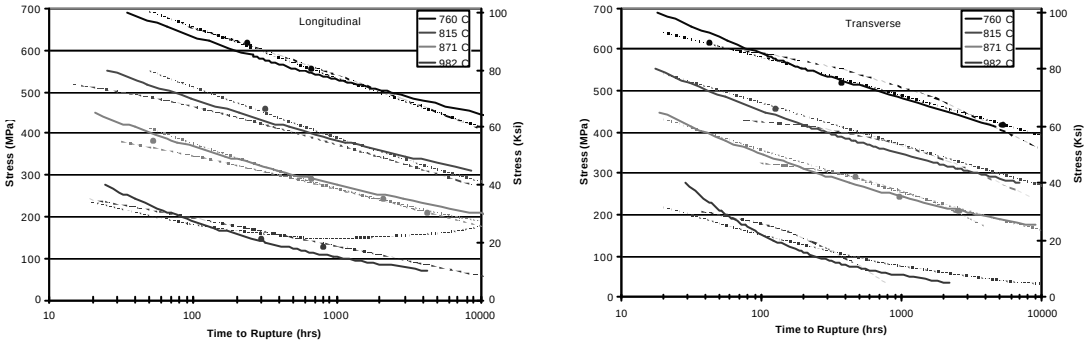

Figure 2: Stress versus Time to rupture for DS GTD111. Circles represent experimental points. Solid lines: power law creep model coupled with Monkman-Grant rupture criterion. Dotted lines: *LMP*. Dashed lines: *q*-projection.

3.2 Creep Crack Growth

The *da/dt* and corresponding C_t values are shown in Figure 4. The creep crack growth behavior of LT and TL specimens at 760°C and 871°C were very comparable, even though the crack advanced more rapidly in the TL orientation and at higher temperatures. A single regression line was fitted through the data for both orientations and temperatures. The fitted creep crack growth behavior is described by eqn. (4), where, *da/dt* is expressed in *mm/hr* and C_t in *KN/m-hr*

$$\frac{da}{dt} = 0.050 C_t^{1.04} \tag{4}$$

The exponent of the previous equations is close to unity, therefore the relationship between the crack advance rate and C_t can be represented in a simpler way by a linear relationship. In this case the behavior is described by $da/dt = 0.038 C_t$ if da/dt is expressed in *mm/hr* and C_t in *KN/m-hr*

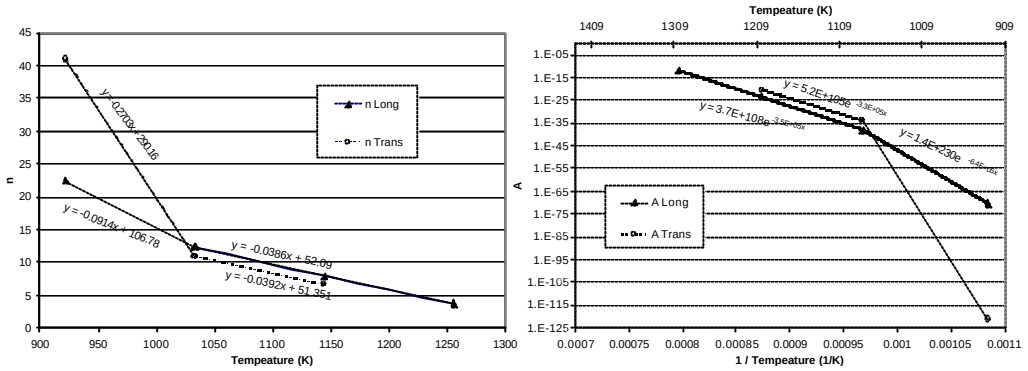

Figure 3: Creep power law coefficient A and creep power law exponent n as a function of temperature. $\dot{e}_{SS} = As^n$.

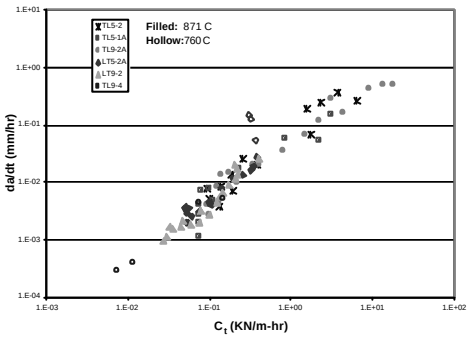

Figure 4: Creep crack growth rate versus C_t obtained experimentally at 871°C and 760°C

4 CONCLUSIONS

The creep deformation and rupture behavior and creep crack growth behavior of a directionally solidified nickel-based superalloy have been characterized and models applied to support remaining-life calculations. The tensile creep behavior consistently shows a very short primary creep regime, followed by a substantial steady-state region that accounts for more than half of the creep life but only between 20 % to 33% of the creep strain. Subsequently, a tertiary creep stage develops that is responsible for less than half of the creep life but for the majority of the accumulated creep strain. The longitudinal orientation shows a longer creep life, larger final

elongation and lower minimum strain rate than the transverse one and than the equiaxed material. The differences become smaller at higher temperatures. The time to rupture for any creep test at any combination of temperature and stress in the range studied can be accurately predicted by the Larson Miller parameter, the rupture model based on secondary power law creep coupled with the Monkman-Grant rupture criterion and by the theta projection model. The creep deformation behavior can be predicted by the power law model and by the theta projection model.

Creep crack growth specimens tested in the LT orientation presented lower crack advance rates than the TL orientation and were completely correlated by C_t. Further, a single relationship between, creep crack growth rate and C_t was applicable to all temperatures and both orientations.

5 REFERENCES.

[1]Woodford, D. and Stiles, D. "High Temperature Performance Evaluation of a Directionally Solidified Nickel-Base Superalloy", Journal of Materials Engineering and Performance, Vol. 6 pp 521-533, 1997.

[2] Trexler, M., and Sanders, T.H., "Prognostics for Gas Turbines Systems Reliability" – 2nd Annual Project Research Report, Part III, Georgia Institute of Technology, 2002.

[3] Riedel, H., "Creep Deformation at Crack Tips in Elastic-Viscoplastic Solids", Journal of Mechanics and Physics of Solids, (29), pp 35-49, 1981.

[4] Staley, J. T., Saxena, A., "Mechanisms of Creep Crack Growth in 1 wt% Antimony-Copper", Acta Metall. Mater., Vol. 38, No. 6, pp. 897-908, 1990.

[5] Monkman, F. and Grant, N., Proc. ASTM, Vol. 56, p595, 1956.

[6] Evans R. and Wilshire B., "Introduction to Creep", The Institute of Materials, pp 64-97, 1993.

[7] Larson, R. and Miller, J, Trans. ASME, Vol. 74, p765, 1952.

[8] Viswanathan, R., "Damage Mechanisms and Life Assessment of High-Temperature Components", ASM International